Interaction of a Bacterial Endotoxin with Different Surfaces Investigated by in Situ Fourier Transform Infrared Attenuated Total Reflection Spectroscopy

G. Reiter,[†] M. Siam,[†] D. Falkenhagen,[‡] W. Gollneritsch,[‡] D. Baurecht,[†] and U. P. Fringeli*,[†]

Institute of Physical Chemistry, University of Vienna, Althanstrasse 14, A-1090 Vienna, Austria, and Center of Biomedical Technology, Danube University, Dr.-Karl-Dorrek-Strasse 30, A-3500 Krems, Austria

Received November 9, 2001. In Final Form: March 22, 2002

The interaction of negatively charged lipopolysaccharide (LPS) from *Pseudomonas aeruginosa* (serotype 10) with different kinds of surfaces was investigated by FTIR ATR spectroscopy. The surfaces comprise a hydrophilic germanium plate, a hydrophobic dipalmitoylphosphatidic acid (DPPA) monolayer, a positively charged cross-linked aminopropyltriethoxysilane (ATS) polymer, and a positively charged lipid bilayer consisting of a DPPA inner monolayer attached to the internal reflection element (IRE) and an outer monolayer consisting of equal molar amounts of palmitoyloleoylphosphatidylcholine (POPC) and hexadecylpyridinium (HDPyr) as positively charged component. Whereas the hydrophilic and negatively charged LPS exhibited only weak adsorption to a hydrophilic Ge IRE and to a hydrophobic DPPA monolayer, it bound strongly to the positively charged surface of ATS and interacted also with the POPC/HDPyr membrane. However, in the latter case, the positively charged component (HDPyr) turned out to be not sufficiently strong anchored in the lipid matrix, because it was completely extracted by the endotoxin. The remaining POPC layer exhibited a significantly reduced molecular ordering compared with a compact POPC monolayer. The results demonstrate distinct interactions of the negatively charged LPS with positively charged surfaces and the ability of LPS to remove positively charged molecules from a biomembrane.

Introduction

Despite the development of broad-spectrum antibiotics, septic shock remains a frequent cause of death, in particular the death of intensive care patients. Septic shock is believed to be a consequence of an excessive production of cytokines such as interleukins and tumor-necrosis factor. Some of the most potent stimulators of the immune system are bacterial lipopolysaccharides (LPSs). They play an important role in the pathogenesis and manifestation of Gram-negative infection, in general, and of septic shock, in particular, and are thus called endotoxins.[1] They can be made responsible for approximately 50% of all sepsis cases.[2,3]

LPSs are complex lipid-linked carbohydrates which are found in the outer membranes of Gram-negative bacteria. These negatively charged molecules are usually composed of a polymeric carbohydrate (O-antigen), a short oligosaccharide (R-core), and a fatty-acylated region (lipid A). It is known that lipid A, the lipid anchor of LPS to the bacterial outer membrane, with its peculiar chemical structure represents the "endotoxic principle" of LPS and is responsible for the expression of pathophysiological effects.[4−6] Through its action on macrophages, LPS can trigger responses that are protective or injurious to the host.[7]

The physical characterization and elucidation of the function of LPS in the bacterial membrane with respect to its permeation properties, its susceptibility against drugs, and its role in the activation of the immune system have been investigated via electrophysiological experiments with a reconstituted model of the outer membrane as planar asymmetric lipid bilayer.[8] The first successful experiments with Fourier transform infrared (FTIR) spectroscopic methods to study the architecture and dynamics of LPS membranes of living bacteria have already been carried out,[9] as well as investigations into the physicochemical characteristics of lipid A.[10−12] Furthermore, there also exist a variety of FTIR studies on the interaction of LPS or lipid A with soluble proteins (e.g., lipopolysaccharide binding protein,[13] lysozyme[14]). Nevertheless, the molecular mechanisms of action of endo-

[†] University of Vienna.

[‡] Danube University.

(1) Rietschel, E. T.; Brade, H.; Holst, O.; Brade, L.; Müller-Loennies, S.; Mamat, U.; Zähringer, U.; Beckmann, F.; Seydel, U.; Brandenburg, K.; Ulmer, A. J.; Mattern, T.; Heine, H.; Schletter, J.; Hauschildt, S.; Loppnow, H.; Schönbeck, U.; Flad, H.-D.; Schade, U. F.; Di Padova, S.; Kusumoto, S.; Schumann, R. R. *Curr. Top. Microbiol. Immunol.* **1996**, *216*, 39.

(2) Rietschel, E. T.; Brade, H.; Brade, L.; Brandenburg, K.; Schade, U.; Seydel, U.; Zähringer, U.; Galanos, C.; Lüderitz, O.; Westphal, O.; Labischinski, H.; Kusumoto, S.; Shiba, *T. Prog. Clin. Biol. Res.* **1987**, *231*, 25.

(3) Hurley, J.; Levin, J. In *Endotoxin in Health and Disease*; Morrison, D. C., Brade, H., Opal, S., Vogel, S., Eds.; Marcel Dekker: New York, 1999; p 841.

(4) Rietschel, E. T.; Brade, H.; Brade, L.; Brandenburg, K.; Schade, U.; Seydel, U.; Zähringer, U.; Galanos, C.; Lüderitz, O.; Westphal, O.; Labischinski, H.; Kusumoto, S.; Shiba, T. *Prog. Clin. Biol. Res.* **1987**, *231*, 25.

(5) Brandenburg, K.; Seydel, U.; Schromm, A. B.; Loppnow, H.; Koch, M. H. J.; Rietschel, E. T. *J. Endotoxin Res.* **1996**, *3*, 173.

(6) Seydel, U.; Schromm, A. B.; Blunck, R.; Brandenburg, K. In *Role of CD14 in the Inflammatory Response*; Jack, R., Ed.; Karger: Basel, 2000; p 5.

(7) Sweet, M. J.; Hume, D. A. *J. Leukocyte Biol.* **1996**, *60*, 8.

(8) Seydel, U.; Schröder, G.; Brandenburg, K. *J. Membr. Biol.* **1989**, *109*, 95.

(9) Naumann, D.; Schultz, C.; Sabisch, A.; Kastowsky, M.; Labischinski, H. *J. Mol. Struct.* **1989**, *214*, 213.

(10) Brandenburg, K.; Lindner, B.; Schromm, A.; Koch, M. H. J.; Bauer, J.; Merkli, A.; Zbaeren, C.; Davies, J. G.; Seydel, U. *Eur. J. Biochem.* **2000**, *267*, 3370.

(11) Labischinski, H.; Naumann, D.; Schultz, C.; Kusumoto, S.; Shiba, T.; Rietschel, E. T.; Giesbrecht, T. *Eur. J. Biochem.* **1989**, *179*, 659.

(12) Brandenburg, K.; Seydel, U. *Eur. J. Biochem.* **1988**, *16*, 83.

10.1021/la011662k CCC: $22.00
Published on Web 06/22/2002

toxin, either as an integral component of the bacterial membrane or as a freely administered substance, on the plasma membrane of the host cells leading to the induction of infect-related symptoms are, by far, not comprehensively explored. It was found that the molecular conformation of the lipid A portion of endotoxin has an essential impact on the interaction between endotoxin and host cells.[15]

Pseudomonas aeruginosa is an opportunistic human pathogen that can cause fatal infections, including those with severe burn wounds, cystic fibrosis, and cancer. The pathogenic potency of this bacteria, which is resistant to a great variety of antibiotics, is probably due to special properties and the physical chemistry of its outer membrane, in particular its LPS component. One possible therapeutical approach against *Pseudomonas* infections is the production of broadly cross-protective monoclonal antibodies.[16]

Another approach is the removal of its endotoxin from blood. To get more insight into the mechanisms of blood purification[17] and toxic action, Fourier transform infrared attenuated total reflection (FTIR ATR) spectroscopy[18−22] was used to investigate in situ the interactions of LPS from *Pseudomonas aeruginosa* (serotype 10) with different kinds of surfaces: a hydrophilic germanium (Ge) plate, a hydrophobic monolayer consisting of dipalmitoylphosphatidic acid (DPPA), a positively charged cross-linked γ-aminopropyltriethoxysilane (ATS) polymer, and, finally, a positively charged bilayer consisting of DPPA as inner and a (1:1) mixture of palmitoyloleoylphosphatidylcholine (POPC) and hexadecylpyridinium (HDPyr) as outer leaflet. Instead of HDPyr, hexadecylamine (HDA) and hexadecyltrimethylammonium (HDTMA) were also used as positively charged lipids; however, these results are not presented in this paper, because they were quite similar to those obtained with HDPyr.

Experimental Section

Chemicals and Biochemicals. Water was ultrapure (Elga). In all experiments, the same phosphate buffer (20 mM Na_2HPO_4/NaH_2PO_4, pH 7, 100 mM NaCl, and 0.1 mM $CaCl_2$) was used. The subphase in the LB trough was a 0.1 mM $CaCl_2$ solution. LPS from *Pseudomonas aeruginosa* (serotype 10) (Sigma, L-7018) and POPC were purchased from Sigma. DPPA, HDPyr, HDA, HDTMA, and ATS were purchased from Fluka AG. Chemicals were used without further purification. LPS as received (lyophilisate from trichloroacetic acid extraction, 1−10% protein content) turned out to be contaminated with surface-active proteins not specified by the supplier (see below). Despite this contamination, this LPS charge was used because of its clinical significance. LPS solutions were prepared by vortexing.

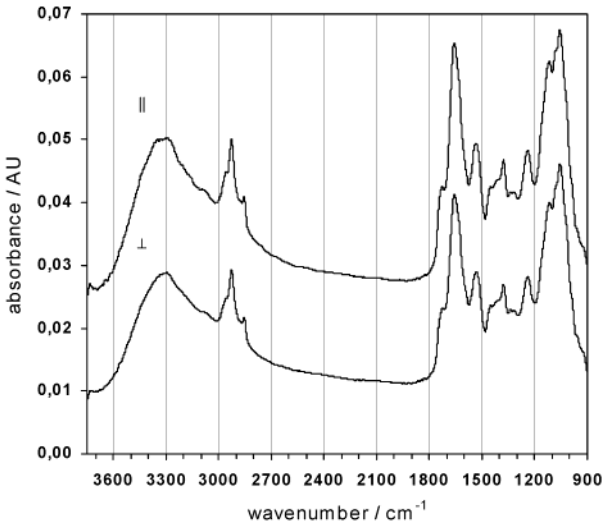

Figure 1. FTIR ATR absorbance spectra of a dry LPS film of *Pseudomonas aeruginosa* (serotype 10), measured with parallel (||) and perpendicular (⊥) polarized incident light. Ge IRE; $T \sim 30$ °C; angle incidence $\Theta = 45°$; number of active internal reflections $N = 22 \pm 2$. Reference: dry Ge IRE.

Sample Preparation. *1. Clean Ge Surface.* Before a new experiment was begun, each side of the Ge ATR plate was machine polished (Logitech PM5) with a pellon cloth by means of a 0.25 μm diamond paste, rotating at 30 rpm for 10 min. Subsequently, the plate was subjected to various cleaning procedures, using consecutively acetone, ultrapure water, and ethanol, until there were no visible impurities left. To remove small traces of organic compounds, all glassware and ATR plates were finally cleaned 3 min by plasma (Harrick Sci. Corp.) before use. The Ge plate was considered to be clean if the $\nu(CH_2)$ bands at ~2920 and ~2850 cm^{-1} disappeared completely in the FTIR ATR spectrum (single-beam mode).

2. LPS Film. The endotoxin film was prepared by spreading an aqueous LPS solution (1 mg of LPS/mL) in ultrapure water on the ATR plate and evaporating the excess water with a nitrogen stream at room temperature. The plate was further dried in the FTIR spectrometer where the decrease of the absorbance of bound water at 3400 and 1640 cm^{-1} was monitored. When no further decrease was detected, spectra of the film were recorded. Typical spectra of a dry LPS layer of *Pseudomonas aeruginosa* (serotype 10) are shown in Figure 1.

3. DPPA Monolayer. A DPPA monolayer was spread at the air−water interface of a film balance (Nima Technology Ltd., The Science Park, Coventry, CV4 7EZ, England) and compressed to a surface pressure of 30 ± 0.2 mN/m. The subphase contained 0.1 mM $CaCl_2$ and was kept at 23 ± 2 °C. Stability of the compressed film was checked and turned out to be complete during the period required for film transfer. A Ge internal reflection plate (IRE) was dipped into the subphase before compressing. Monolayer transfer was performed according to the method of Blodgett and Langmuir[23] and is referred to as LB layer further on. The transfer rate was 2 mm/min, corresponding to an area transfer of 0.84 cm^2/min. The transfer ratio was 1.00 ± 0.03. After withdrawal of the IRE, the DPPA coated part was completely hydrophobic. Typical spectra of a dry DPPA monolayer are shown in Figure 2A.

4. Bilayer Membranes. The bilayer consisting of DPPA as inner and a (1:1) mixture of POPC and HDPyr as outer monolayer (Figure 2B) was prepared using the Langmuir−Blodgett (LB)/vesicle method.[19,24] First, a DPPA monolayer was transferred to the ATR plate as described in the preceding section. Then the

(13) Gutsmann, T.; Schromm, A. B.; Koch, M. H. J.; Kusumoto, S.; Fukase, K.; Oikawa, M.; Seydel, U.; Brandenburg K. *Phys. Chem. Chem. Phys.* **2000**, *2*, 4521.

(14) Brandenburg, K.; Koch, M. H. J.; Seydel, U. *Eur. J. Biochem.* **1998**, *258*, 686.

(15) Schromm, A. B.; Brandenburg, K.; Loppnow, H.; Moran, A. P.; Koch, M. H. J.; Rietschel, E. T.; Seydel, U. *Eur. J. Biochem.* **2000**, *267*, 2008.

(16) Carballo, P. S.; Rietschel, E. T.; Zähringer, U. In *Annual Report 1999*; Board of Directors of Research Center Borstel: Borstel, Germany, 1999, p 299.

(17) Weber, C.; Stummvoll, H. K.; Passon, S.; Falkenhagen, D. *Int. J. Artif. Organs* **1998**, *21*, 335.

(18) Harrick, N. J. *Internal Reflection Spectroscopy*; Harrick Sci. Corp.: Ossining, NY, 1979.

(19) Fringeli, U. P. In *Internal Reflection Spectroscopy*; Mirabella, F. M., Ed.; Marcel Dekker: New York, 1992; pp 255−324.

(20) Fringeli U. P. ATR and Reflectance IR Spectroscopy, Applications. In *Encyclopedia of Spectroscopy and Spectrometry*; Lindon, J. C., Tranter, G. E., Holmes J. C., Eds.; Academic Press: San Diego, 1999; pp 58−75.

(21) Fringeli, U. P.; Baurecht, D.; Günthard Hs. H. Biophysical Infrared Modulation Spectroscopy. In *Infrared and Raman Spectroscopy of Biological Materials*; Gremlich H. U., Yan, B.,Eds.; Marcel Dekker: New York, 2000; pp 143−192.

(22) Fringeli, U. P.; Baurecht, D.; Bürgi, T.; Siam, M.; Reiter, G.; Schwarzott, M.; Brüesch, P. ATR Spectroscopy of Thin Films. In *Handbook of Thin Films Materials*; Nalwa, H. S., Ed.; Academic Press: New York, October 2002; Vol. 2, Chapter 4, pp 191−229.

(23) Blodgett, K. B.; Langmuir, I. *Phys. Rev.* **1937**, *51*, 964.

(24) Wenzl, P.; Fringeli, M.; Goette, J.; Fringeli, U. P. *Langmuir* **1994**, *10*, 4253.

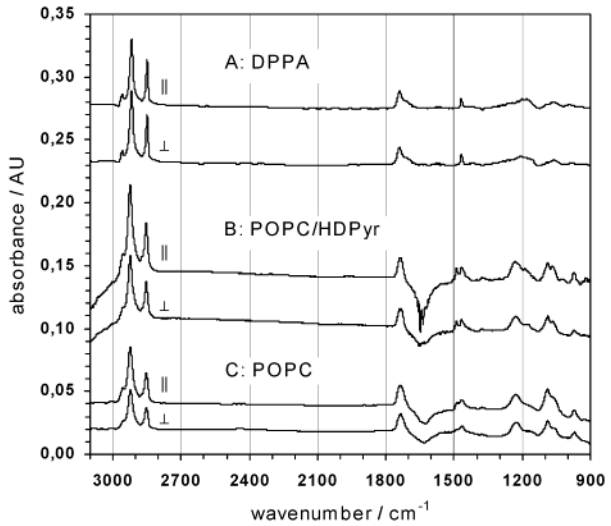

Figure 2. FTIR ATR absorbance spectra measured with parallel (∥) and perpendicular (⊥) polarized incident light. (A) Dry DPPA LB monolayer transferred to a Ge IRE at 30 mN/m from an aqueous subphase containing 10^{-4} M $CaCl_2$. Transfer ratio 1.00 ± 0.03. Surface concentration $\Gamma = 3.79 \times 10^{-10} \pm 0.24 \times 10^{-10}$ mol cm^{-2} (eq 7) using $\nu_s(CH_2)$ at 2850 cm^{-1}. Mean segmental order parameter $\bar{S}_{CH_2} = -0.50 \pm 1.9 \times 10^{-3}$. This DPPA monolayer featured a nearly perfect alignment of all-trans hydrocarbon chains along the normal to the IRE (*z*-axis). Reference: dry Ge IRE. (B) DPPA/(POPC:HDPyr; 1:1 *x*/*x*) bilayer in contact with buffer. Reference: DPPA LB monolayer in contact with buffer. (C) DPPA/POPC bilayer in contact with buffer. Reference: DPPA LB monolayer in contact with buffer. Ge IRE; $T = 25$ °C; angle incidence $\Theta = 45°$; number of active internal reflections $N = 41 \pm 1$ for (A) and $N = 36.6 \pm 1$ for (B) $N = 18.3$ for (C). Buffer for (B) and (C): 20 mM sodium phosphate, pH 7.0, 100 mM NaCl.

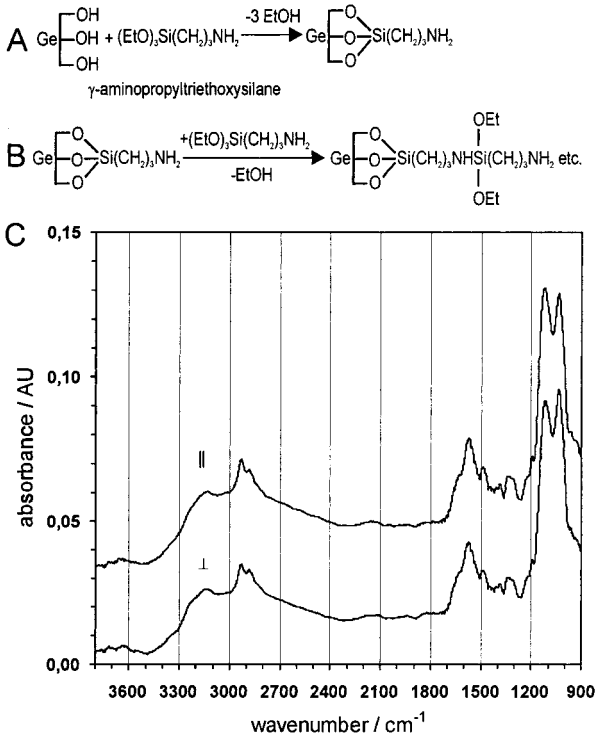

Figure 3. γ-Aminopropyltriethoxysilane (ATS) on a Ge IRE. (A) Reaction of ATS with the hydroxyl groups of a Ge surface. (B) Polymerization reaction between a free ATS and an ATS already bound to the Ge IRE. (C) FTIR ATR absorbance spectra of a ATS polymer network in contact with dry air measured with parallel (∥) and perpendicular (⊥) polarized incident light. Reference: Ge IRE in contact with dry air. Ge IRE; $T \sim 30$ °C; angle incidence $\Theta = 45°$; number of active internal reflections $N \sim 50$.

coated dry plate was mounted in a liquid sample cell for flow-through experiments. The transfer of the second monolayer made use of the energetically unfavorable state of the hydrophobic surface of the DPPA monolayer in contact with the aqueous phase in the sample cell. Completion of the bilayer was therefore performed by spontaneous adsorption of phospholipids from the vesicular solution. This solution was obtained in the following way: POPC and HDPyr were dissolved in chloroform and mixed together in a tube. The chloroform was then evaporated under nitrogen flow and the remaining solid suspended in phosphate buffer (1 mg (total weight) per mL of POPC and HDPyr, 1:1 *x*/*x*, in phosphate buffer). Vesicles were prepared by sonication in N_2 atmosphere at 45 °C. After 20−30 min, the solution was almost completely transparent and was used for the preparation of the second monolayer. This process was monitored in situ by FTIR ATR spectroscopy. The adsorption stopped after completion of the outer leaflet within a maximum of 15 min. After 1 h of contact, the vesicle solution was exchanged by phosphate buffer by pumping 20 mL of buffer solution through the compartments. Now, the asymmetric DPPA/(POPC:HDPyr) bilayer was ready for interaction studies with LPS. Typical spectra of this (POPC:HDPyr) monolayer are shown in Figure 2B, whereas corresponding spectra of a pure POPC monolayer are shown for comparison in Figure 2C. Bilayers containing HDA and HDTMA as positively charged lipids instead of HDPyr have been prepared in the same way; however, the data are not shown in this paper, because they resulted in the same conclusions as drawn from DPPA/(POPC:HDPyr) bilayers.

Finally, a DPPA monolayer was exposed for 25 min to a sonicated POPC:LPS (3:1 *x*/*x*) mixture at 45 °C. The aim of this experiment was to find out whether vesicles consisting of POPC:LPS would also adsorb to the hydrophobic surface of the DPPA LB layer, as pure POPC vesicles do spontaneously.

5. ATS polymer. A positively charged cross-linked polymer consisting of ATS was prepared by polymerization of ATS at the Ge surface in toluene. The scheme is shown in Figure 3A,B. The reaction mixture was composed of 0.3% silane in 120 mL of anhydrous toluene dried by sodium. The reaction time at 100 °C was 10 h. This method of silanization resulted in an ATS polymer network with a thickness depending on the reaction time.[25] The coated plate was transferred into a flow-through cell, and loosely bound parts of ATS were washed out with buffer until there was no detectable decrease of the absorbance of the ν(Si−O) vibrations in the 1000−1200 cm^{-1} range. Typical spectra of an ATS polymer in contact with dry air are shown in Figure 3C.

Spectra Acquisition and Sample Manipulation. *1. FTIR ATR Equipment.* The internal reflection elements (IRE) used for all experiments were 50 × 20 × 1 mm^3 Ge trapezoids with an angle of incidence of $\Theta = 45°$. FTIR spectra were recorded with a Bruker IFS 25 spectrometer equipped with a gold grid polarizer on a KRS-5 substrate. A mercury−cadmium telluride (MCT) detector was used. All spectra were scanned at 2 cm^{-1} resolution using a single-beam-sample-reference (SBSR) ATR attachment.

2. SBSR Method. Sample and reference were placed above each other on either side of the IRE. To get IR spectra from both, a parallel beam was passed alternatively through the sample (S) at the lower half of the IRE and the reference (R) at the upper half of the ATR plate. As S and R are accessible at any time by the single beam of the instrument, this method is referred to as the single-beam-sample-reference (SBSR) technique.[19,20,22,26,27] The resulting spectra, i.e., S/R and −log(S/R), are called SBSR transmittance and absorbance spectra, respectively. A hydrodynamically optimized SBSR cell (flow-through cuvette) made of Delrin was used.[27]

3. Sample Manipulation. In the sample cuvette of the SBSR ATR cell, the surfaces under consideration were brought in

(25) Hofer, P.; Fringeli, U. P. *Eur. Biophys. J.* **1979**, *6*, 67.
(26) Fringeli, U. P.; Goette, J.; Reiter, G.; Siam, M.; Baurecht, D. Structural Investigations of Oriented Membrane Assemblies by FTIR-ATR Spectroscopy. In *Fourier Transform Spectroscopy: 11th International Conference*; deHaseth, J. A., Ed.; AIP Conference Proceedings 430; American Institute of Physics: Woodbury, NY, 1998; pp 729−747.
(27) SBSR equipment was obtained from OPTISPEC, Rigistrasse 5, CH-8173 Neerach, Switzerland.

Table 1. Magnitudes and Uncertainties of Input Parameters[a]

parameter	symbol	magnitude	uncertainty
angle of incidence/deg	Θ	45.00	1.50
refractive index of Ge IRE	n_1	4.00	0.00
refractive index of membrane	n_2	1.45	0.05
refractive index of aqueous environment at 2850 cm^{-1}	n_3	1.41	0.05
angle between transition moment of $\nu_s(CH_2)$ and local orientation axis[22]/deg		90.0	0.0
integrated absorbance of $\nu_s(CH_2)$ from extracted HDPyr, parallel polarized spectrum[b]/cm^{-1}	$a_{\parallel}$	0.1064	0.005
integrated absorbance of $\nu_s(CH_2)$ from extracted HDPyr, perpendicular polarized spectrum[c]/cm^{-1}	$a_{\perp}$	0.1037	0.005
integrated molar absorption coefficient of $\nu_s(CH_2)$[d]/ (cm/mol)	$\int\epsilon(\tilde{\nu})\,d\tilde{\nu}$	5.70×10^5	2.00×10^4
integrated molar absorption coefficient of amide II[e]/ (cm/mol)	$\int\epsilon(\tilde{\nu})\,d\tilde{\nu}$	8.25×10^6	2.90×10^5
initial distance of HDPyr layer from IRE surface/Å	z_i	25	2
final distance of HDPyr layer from IRE surface/Å	z_f	50	2
number of active internal reflections	N		
HDPyr/POPC interaction with LPS		36.6	1
POPC		18.3	1
number of methylene groups per molecular unit	ν		
HDPyr		15	0
POPC		32	0
POPC/HDPyr complex		47	0

[a] The limit of confidence is approximately 95%. [b] Figure 6. Linear baseline. Range of integration: 2830 ± 1 to 2869 ± 1 cm^{-1}. [c] Figure 6. Linear baseline. Range of integration: 2830 ± 1 to 2869 ± 1 cm^{-1}. [d] Linear baseline. Range of integration: 2830 ± 1 to 2869 ± 1 cm^{-1}. [e] Linear baseline. Range of integration: 1585 ± 1 to 1500 ± 1 cm^{-1}.

contact with aqueous buffer solutions of LPS of increasing concentration (1, 10, 100, 1000 μg/mL) (peristaltic pump with ismaprene tubings). If not otherwise stated, each LPS solution was left in the cell until equilibrium was reached which was the case after about 30 min. Then the system was washed with buffer. During all steps, the reference part of the SBSR cell had to sustain the same procedure with buffer.

4. Integrated Molar Absorption Coefficients. The integrated molar absorption coefficient for the symmetric CH-stretching vibration of methylene groups, $\nu_s(CH_2)$, has been determined via ATR measurements with polarized light using a DPPA monolayer transferred to the IRE at 30 mN/m. Calibration was based on the molecular cross section of 0.44 nm^2 of a DPPA molecule as reported in ref 31. The integrated molar absorption coefficient of the amide II vibration of proteins was calibrated indirectly via DPPA from IR ATR measurements of thin films containing DPPA and small peptides with known molar ratios. The values are indicated in Table 1; they have to be considered as conformation-independent mean values. Details will be published elsewhere.

Theoretical Section

Orientation Measurements. Orientation measurements require independent spectra of the sample by means of parallel and perpendicular polarized incident light. To get rid of physical and molecular constants, such as the magnitude of the transition moment, the so-called dichroic ratio $R = a_{\parallel}/a_{\perp}$ is generally used as a basic quantity. $a_{\parallel}$ and $a_{\perp}$ denote the integrated absorbances of measured spectra with parallel and perpendicular polarized incident light. It should be mentioned that peak absorbances may also be used instead of integrated absorbances. Introducing the relative electric field components E_x, E_y, and E_z as obtained from Fresnel's equations[18,19] and assuming a liquid crystalline ultrastructure (LCU) of the sample, one obtains for the dichroic ratio the expression

$$R = \frac{a_{\parallel}}{a_{\perp}} = \frac{E_x^2}{E_y^2} + 2\frac{E_z^2}{E_y^2}\frac{\overline{\langle\cos^2\theta\rangle}}{1 - \overline{\langle\cos^2\theta\rangle}} \qquad (1)$$

$\overline{\langle\cos^2\theta\rangle}$ denotes the average over the mean squares of the cosines of the angles between the transition moments of a given vibration and the z-axis of the laboratory coordinate system, which is fixed to the internal reflection element (IRE). The xy-plane is parallel to the surface of the IRE, and the x-axis is aligned along the direction of light propagation. The z-axis is perpendicular to the IRE surface. Obviously, the dichroic ratio R is experimentally directly accessible, while the relative electric field components E_x, E_y, and E_z have to be calculated by means of Fresnel's equations.[18,19]

Solving eq 1 for the mean square cosine results in

$$\overline{\langle\cos^2\theta\rangle} = \frac{E_x^2 - RE_y^2}{E_x^2 - RE_y^2 - 2E_z^2} \qquad (2)$$

Information on the mean orientation of transition moments may also be expressed in terms of order parameters. The mean segmental order parameter of the kth vibrational mode of a system, $\bar{S}_k$, is related to the mean square cosine by

$$\bar{S}_k = \frac{3}{2}\overline{\langle\cos^2\theta_k\rangle} - \frac{1}{2} \qquad (3)$$

It should be noted for completeness that, to derive information on the flexibility of a molecular segment from the results obtained by eq 2 or 3, it is necessary to make use of a model probability density function.[19]

Three special cases of molecular orientation should be mentioned here: the isotropic arrangement of transition dipole moments, resulting in $\overline{\langle\cos^2\theta_k\rangle}_{iso} = 1/3$, thus $\bar{S}_{k,iso} = 0$; the perfect alignment of the transition dipole moments parallel to the surface of the IRE (xy-plane), resulting in $\overline{\langle\cos^2\theta_k\rangle}_{xy} = 0$ and $\bar{S}_{k,xy} = -1/2$; and perfect alignment of transition moments along the normal to the IRE (z-axis), resulting in $\overline{\langle\cos^2\theta_k\rangle}_z = 1$ and $\bar{S}_{k,z} = 1$, respectively. As can be derived from eq 1, the corresponding dichroic ratios are

$$R_{iso} = \frac{E_x^2 + E_z^2}{E_y^2}, R_{xy} = \frac{E_x^2}{E_y^2}, \quad R_z = \infty$$

A situation often encountered with larger molecules is the existence of several populations of equal functional groups, featuring different orientational ordering. Con-

(28) Seelig, J. *Q. Rev. Biophys.* **1977**, *10*, 353.
(29) Zurmühl, R. *Praktische Mathematik für Ingenieure und Physiker*; Springer-Verlag: Berlin, Heidelberg, New York, 1965.
(30) The MathWorks, Inc., 24 Prime Park Way, Natick, MA 01760.
(31) Demel, R. A.; Yin, C. C.; Lin, B. Z.; Hauser, H. *Chem. Phys. Lipids* **1992**, *60*, 209.

sider, e.g., the 32 methylene groups of POPC. Fourteen CH_2 groups are located in each of the two hydrocarbon chains. Both the glycerol moiety and the choline headgroup contain a further two CH_2 groups. Strictly speaking, each single group is characterized by its own mean square cosine $\langle\cos^2\theta_k\rangle$, where $k = 1, 2, ..., 32$. Corresponding vibrations, such as $\nu_s(CH_2)$ at $\sim$2850 cm^{-1}, will therefore lead to heavily overlapped absorption bands, because generally only small frequency shifts occur with respect to the band positions. As a consequence, only mean absorbances are accessible, resulting in mean dichroic ratios, unless molecules with selectively deuterated methylene groups are used. Detailed information on methylene group flexibilities in phospholipids has been reported by Seelig[28] using deuterium NMR applied to selectively deuterated lipids.

Considering now a superimposed absorption band resulting from a distinct group vibration (e.g., $\nu_s(CH_2)$), and assuming N populations of this group featuring different mean orientations in space, the resulting dichroic ratio can then be expressed as follows:[19,22]

$$\langle R\rangle = \frac{\sum_{k=1}^{N} x_k {m_k}^2 \langle d_{e,k\parallel}\rangle}{\sum_{k=1}^{N} x_k {m_k}^2 \langle d_{e,k\perp}\rangle} \tag{4}$$

The index k stands for the kth population of the functional group. x_k, m_k, $\langle d_{e,k\parallel}\rangle$ and $\langle d_{e,k\perp}\rangle$ denote mole fraction, relative magnitude of the transition moment M_k, where $k = 1, ..., N$ ($m_k = M_k/M_1$), and effective thicknesses for parallel and perpendicular polarized incident light, respectively. Equation 4 is equivalent to eq 34 in ref 19. The effective thicknesses are composed of the axial contributions which depend on the corresponding effective thickness of an isotropic sample as well as on the mean square cosine according to eqs 5.

$$\langle d_{e,k\parallel}\rangle = \langle d_{e,k,x}\rangle + \langle d_{e,k,z}\rangle = 3\left[\frac{1}{2}\langle d_{e,x}\rangle_{iso} + \langle\cos^2\theta_k\rangle\left(\langle d_{e,z}\rangle_{iso} - \frac{1}{2}\langle d_{e,x}\rangle_{iso}\right)\right]$$

$$\langle d_{e,k\perp}\rangle = \langle d_{e,k,y}\rangle\frac{3}{2}(1 - \langle\cos^2\theta_k\rangle)\langle d_{e,y}\rangle_{iso} \tag{5}$$

Note that $\langle\cos^2\theta_k\rangle = 1/3$ for an isotropic sample.

The reader is referred to refs 18, 19, and 22 for explicit expressions of effective thicknesses. To give an idea on the magnitude of effective thicknesses, numerical values will be given here for a special application in this paper.

The following values of relevant parameters have been used: angle of incidence $\theta = 45° \pm 1.5°$; refractive indices of Ge IRE, supported lipid layer, and buffer solution were $n_1 = 4.0$, $n_2 = 1.45 \pm 0.05$, and $\bar{n}_3 = 1.41 \pm 0.05$ (note that anomalous dispersion of water at 2850 cm^{-1} has been taken into account; $n_3 = 1.33$ is valid outside of strong water absorption). Based on these optical constants and the thin film approximation theory,[18] the components of the relative electric field strength in the rarer medium resulted in $E_x = 1.400 \pm 0.002$, $E_y = 1.511 \pm 0.008$, and $E_z = 1.527 \pm 0.162$. The corresponding axial effective thicknesses for an isotropic thin layer were then calculated to be $\langle d_{e,x}\rangle_{iso} = 2.51 \pm 0.30$ nm, $\langle d_{e,y}\rangle_{iso} = 2.93 \pm 0.36$ nm, and $\langle d_{e,z}\rangle_{iso} = 2.99 \pm 0.73$ nm. Thus one obtains for an isotropic arrangement of molecules in a thin film a dichroic ratio of $R_{iso} = (\langle d_{e,x}\rangle_{iso} + \langle d_{e,z}\rangle_{iso})/\langle d_{e,y}\rangle_{iso} = 1.88 \pm 0.22$, while for perfect alignment of the transition moments parallel to the IRE surface (xy-plane) the dichroic ratio would result in $R_{xy} = 0.858 \pm 0.009$; see also Table 1.

Determination of Volume Concentration and Surface Concentration. The quantities volume concentration c and the surface concentration Γ are related to each other via the thickness of the sample d and the Lambert−Beer law by

$$c = \frac{\Gamma}{d} = \frac{a_\perp}{N\nu d_{e,\perp}\int\epsilon(\tilde{\nu})\,d\tilde{\nu}} \tag{6}$$

where $a_\perp$ denotes the integrated absorbance of a given absorption band measured with $\perp$-polarized light; N and ν are the mean number of active internal reflections and the number of equal functional groups (e.g., methylene groups) per molecule. The effective thickness of an arbitrary oriented sample per internal reflection is denoted by $d_{e,\perp}$, whereas $d_{e,\perp}^{iso}$ is the effective thickness for an isotropic sample. $\int\epsilon(\tilde{\nu})\,d\tilde{\nu}$ denotes the integrated molar absorption coefficient of this band.

According to eq 6 Γ may be understood as the projection of the molecules in the volume defined by the unit area and the height d, which is equivalent to the real sample thickness. Then

$$\Gamma = \frac{a_\perp}{N\nu d_{e,\perp}^{rel}\int\epsilon(\tilde{\nu})\,d\tilde{\nu}} = \frac{a_\perp}{3N\nu d_{e,\perp}^{rel,iso}\int\epsilon(\tilde{\nu})\,d\tilde{\nu}}\left[2 - \frac{{E_x}^2}{{E_z}^2} + R\frac{{E_y}^2}{{E_z}^2}\right] \tag{7}$$

The right-hand side of eq 7 is based on the assumption of a liquid crystalline ultrastructure (LCU),[24] as well as on the thin film approximation.[18] In the thin film approximation, the effective thickness becomes directly proportional to the real thickness d. As a consequence, the relative effective thickness $d_{e,\perp}^{rel}$ as defined by eq 8 becomes independent of the real sample thickness d.

$$d_{e,\perp}^{rel} = \frac{d_{e,\perp}}{d} \tag{8}$$

In a more recent review article[22] it was shown that eqs 1−8, which are based on the thin film and the weak absorber approximations, originally introduced by Harrick,[18] are in excellent agreement with straightforward accurate ATR data analysis, as long as the product of the absorption coefficient α per internal reflection, and the effective thickness d_e, i.e., $\alpha = \epsilon d_e \leq 0.1$. This condition is fulfilled even for many bulk organic and inorganic media. However, more sophisticated theoretical approaches must be used, when thin metal layers are part of the assembly.

Error Analysis. The uncertainties indicated in this section and later on in this paper are all based on a straightforward error propagation calculation.[29] Analytical expressions for partial derivatives have been evaluated by means of the Symbolic Mathematical Toolbox of MATLAB,[30] whereas the final numeric calculation of overall uncertainties has been performed by means of the standard MATLAB software. The uncertainties of the input parameters are presented in Table 1. They correspond to approximately a 95% limit of confidence.

Results

Characterization of Surfaces Used for LPS Interaction. *1. Hydrocarbon Chains of a DPPA Monolayer.* A DPPA LB monolayer was transferred from the air−water

interface to a germanium (Ge) IRE. Clean Ge has a hydrophilic surface like glass, thus attaching the polar headgroups of a spread lipid during withdrawing of the plate from the subphase through the compressed film. As a consequence, the new surface is hydrophobic. Typical absorbance spectra from a dry monolayer obtained with polarized incident light are shown in Figure 2A. The most prominent absorption bands are found at 2917 and 2850 cm^{-1}. They result from asymmetric, $\nu_{as}(CH_2)$, and symmetric, $\nu_s(CH_2)$, CH stretching of the methylene groups. Corresponding weaker bands from methyl groups are located at 2959 cm^{-1}, $\nu_{as}(CH_3)$, and at about 2873 cm^{-1}, $\nu_s(CH_3)$, which, however, is only visible as a very weak parallel polarized hump. C═O stretching from the two fatty acid ester groups resulted in two absorption bands, a sharp one at 1740 cm^{-1} and a rather broad one at 1715 cm^{-1}. This prominent splitting gives evidence of the nonequivalence of structures and/or surroundings of the neighboring ester groups. In this experimental series the surface concentration of DPPA as calculated from the absorbances of the symmetric CH_2 stretching according to eq 7 is found to be $\Gamma = 3.79 \times 10^{-10} \pm 0.24 \times 10^{-10}$ mol cm^{-2}. This surface concentration corresponds to 43.8 ± 2.6 $Å^2$/molecule, which is in very good agreement with 43.8 $Å^2$/molecule as reported by Demel et al.[31] for DPPA in a monolayer at the air/water interface at pH 7.2 and a surface pressure above 30 mNm^{-1}.

2. Bilayers. The absorbance spectra of the outer monolayer of the positively charged bilayer DPPA/(POPC:HDPyr; 1:1 *x*/*x*) are shown in Figure 2B. The reference was a DPPA LB layer in contact with the same buffer. Since HDPyr has no fatty acid ester group, the C═O-stretching vibrations near 1740 cm^{-1} can be used as a marker band for POPC. Furthermore, a weak and narrow absorption band near 1500 cm^{-1} can be associated with C═C stretching of the aromatic pyridinium ring of HDPyr.

Endotoxin membrane interaction will essentially be documented by experiments performed with a DPPA/(POPC:HDPyr; 1:1 *x*/*x*) bilayer, because the influence of LPS on the other two positively charged bilayers (POPC:HDA; 1:1 *x*/*x* and POPC:HDTMA; 1:1 *x*/*x*) was analogous.

3. ATS. The absorbance spectrum of a positively charged cross-linked aminopropyltriethoxysilane (ATS) polymer is shown in Figure 3C. Si−O−C, Si−O−Ge, and N−Si−O stretching is involved in the two dominating bands at 1125 and 1030 cm^{-1}.[33] Absorption bands resulting from symmetric and asymmetric CH_2 stretching of the propyl group are located near 2870 and 2925 cm^{-1}. The bands near 3200 and 1600 cm^{-1} are assigned to vibrations with NH stretching and NH bending involved, respectively.

LPS Interaction. For comparison, the spectra of a dried film of the LPS used in these experiments are shown in Figure 1. A detailed interpretation of the IR spectra of various endotoxins has already been given by other research groups.[5−15] To quantify bound LPS, we focused on the typical stretching vibrations of the sugar moieties (ν(CO) between 900 and 1100 cm^{-1}) and the phosphate groups of the lipid A part ($\nu_s(PO_2^{2-})$ near 1100 cm^{-1} and $\nu_{as}(PO_2^{2-})$ near 1250 cm^{-1}).

It should be noted that, in comparison with spectra of other endotoxins investigated by FTIR spectroscopy,[5−15] the amide bands of our LPS appear significantly more intense. As has turned out in the course of our experiments,

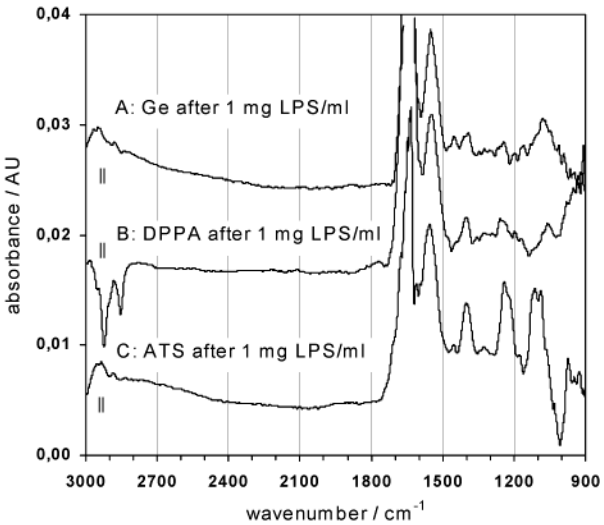

Figure 4. FTIR ATR absorbance spectra of *Pseudomonas aeruginosa* (LPS) interacting with different surfaces measured with parallel (∥) polarized incident light. A solution of 1 mg/mL LPS in buffer was pumped through the ATR cuvette. Equilibrium was reached after a few minutes. Then the LPS solution was replaced by buffer. Tightly bound LPS may be monitored by the asymmetric stretching vibration of the phosphate group of the lipid A moiety, $\nu_{as}(PO_2^-)$, at ∼1250 cm^{-1}. Huge amide I and amide II bands resulting from a highly surface active protein contaminant in the supplied LPS sample are observed with every surface. Quantitative analysis reveals, however, that this contaminant could not influence significantly the presented LPS studies; see text. (A) LPS adsorbed to a hydrophilic Ge IRE in contact with buffer. Reference: Ge IRE in contact with buffer. (B) LPS adsorbed to the hydrophobic side of a DPPA LB layer in contact with buffer. The negative CH_2-stretching bands reflect LPS-induced detachment of DPPA. Quantitative analysis revealed about 25% lipid loss. Reference: DPPA LB monolayer in contact with buffer. (C) LPS bound to a positively charged polymer network of ATS in contact with buffer. A significant accumulation is observed, probably by electrostatic interaction between LPS and ATS. Reference: ATS polymer network in contact with buffer. Ge IRE; $T = 25$ °C; angle incidence $\Theta = 45°$; number of active internal reflections $N = 36.6 \pm 1$. Buffer: 20 mM sodium phosphate, pH 7.0, 100 mM NaCl.

this can be explained by a highly surface active protein contaminant, which was accumulated at the surface of the IRE.

1. Interaction of LPS with a Clean Ge IRE, a DPPA Monolayer, and an ATS Polymer Network. Interactions of LPS with a plasma-cleaned, hydrophilic surface of the Ge IRE, with a DPPA monolayer facing its hydrophobic side toward the aqueous phase, and with a supported positively charged ATS polymer, were studied by pumping LPS solutions over these surfaces until adsorption equilibrium was reached. All surfaces have been washed with buffer before recording the spectra, to eliminate loosely bound LPS.

Intense amide I (1640 cm^{-1}) and amide II (1550 cm^{-1}) bands appeared irrespective of the surface. However, the band intensities in the 900−1100 cm^{-1} range reflected a significant dependence on the nature of the exposed surface. The following preferences were found: ATS > Ge > DPPA, as can be concluded from Figure 4. As reported earlier, the intense amide bands resulted predominately from highly surface active protein contaminants in the original LPS sample. LPS did not bind to the hydrophobic surface of DPPA. In contrast, the very tightly packed LB monolayer was destabilized as revealed by a loss of about 25% of DPPA. This is the reason for the negative CH-stretching bands observed in Figure 4B. This effect is not observed when the dissolved LPS is in contact with POPC

(32) Schlegel, H. G. *Allgemeine Mikrobiologie*; Thieme-Verlag: Stuttgart, New York, 1985; p 50.
(33) Bellamy, L. J. *The Infrared Spectra of Complex Molecules*; Methuen: London, 1975.

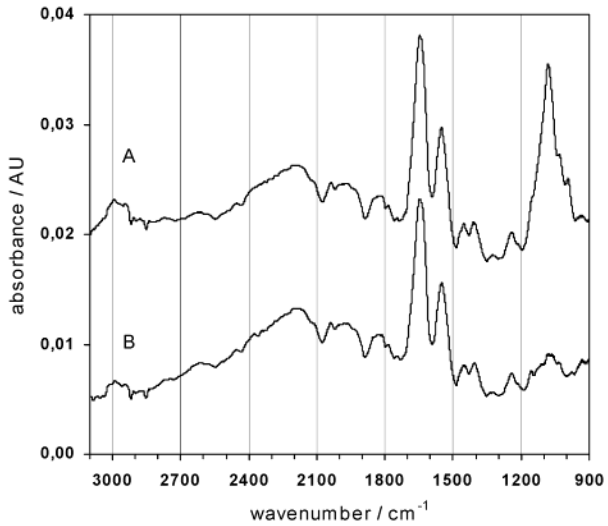

Figure 5. FTIR ATR absorbance spectra of a DPPA LB monolayer interacting with a vesicular solution of POPC:LPS (3:1 *x*/*x*) measured with unpolarized incident light. The mixture consisted of 0.5 mg of POPC and 1.5 mg of LPS per milliliter. Note that, in the absence of LPS, POPC would adsorb spontaneously to the hydrophobic surface of the DPPA layer;[24] however, in the presence of LPS this process is inhibited and just so the detachment of DPPA by pure LPS (see Figure 4B). (A) DPPA LB monolayer in contact with POPC:LPS (3:1 *x*/*x*) in buffer. Reference: DPPA LB monolayer in contact with buffer. (B) DPPA LB monolayer after the interaction with POPC:LPS (3:1 *x*/*x*), now in contact with pure buffer. Reference: DPPA LB monolayer in contact with buffer. Exchange of POPC:LPS (3:1 *x*/*x*) solution by pure buffer led to the detachment of loosely bound LPS; however, the protein contaminant remained tightly bound as revealed by the amide I (1640 cm^{-1}) and amide II (1550 cm^{-1}) bands. Ge IRE; $T = 25$ °C; angle incidence $\Theta = 45°$; number of active internal reflections $N = 36.6 \pm 1$. Buffer: 20 mM sodium phosphate, pH 7.0, 100 mM NaCl.

vesicles. Consequently, a destabilization of the DPPA monolayer by the protein contaminant can be excluded.

The interaction of a sonicated POPC:LPS solution with a DPPA LB monolayer was monitored, too. A pure vesicular POPC solution leads to a spontaneous formation of a DPPA/POPC bilayer; see Figure 2C. However, in the presence of LPS, POPC was hindered from adsorbing to the hydrophobic surface of the DPPA monolayer. Instead of POPC the strong amide bands of the protein contaminant appeared. They were paralleled by typical bands of LPS as shown by Figure 5A. Figure 1 can be used to identify typical LPS absorption bands. However, LPS turned out to be only loosely bound to the DPPA monolayer surface, because after exchanging the POPC/LPS solution by pure buffer, the sugar and phosphate vibrations in the range of 900−1250 cm^{-1} vanished almost completely as shown by Figure 5B, whereas the amide I and II bands at 1640 and 1550 cm^{-1} remained, indicating again the persistence of the highly surface active protein contaminant. It should be noted that in the presence of POPC there was no DPPA destabilization observed.

The highest amount of bound LPS was observed with the positively charged polymer network of ATS, Figure 4C. This effect resulted most probably from electrostatic interaction of ATS with the negatively charged LPS.

2. Interaction of LPS with a DPPA/(POPC:HDPyr) Bilayer.

Figure 6 shows the influence of increasing LPS concentrations on a DPPA/(POPC:HDPyr) bilayer, which was attached to a Ge IRE. Three parallel polarized absorbance spectra are associated with each concentration. A perpendicular polarized SBSR spectrum from the membrane

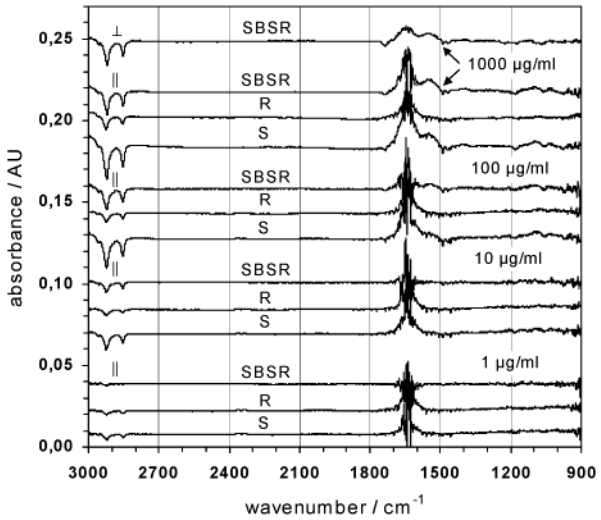

Figure 6. FTIR ATR absorbance spectra of a DPPA/(POPC:HDPyr) (1:1 *x*/*x*) bilayer interacting with increasing concentrations of LPS (from bottom to top) measured with parallel (||) polarized incident light after 30 min of interaction with LPS in each case. A SBSR spectrum measured with perpendicular (⊥) polarized light with the highest LPS concentration is shown on top. Reference: DPPA/(POPC:HDPyr) (1:1 *x*/*x*) bilayer in contact with pure buffer. (S, R) Absorbance spectra measured in the sample and reference channels of the SBSR flow-through cuvette, respectively, using single channel reference spectra stored before the beginning of LPS application in the S-channel. (SBSR) Difference absorbance spectra S − R accumulated in the SBSR scanning mode. SBSR spectra reflect the actual difference between a sample and a reference of approximately the same age, since the DPPA/(POPC:HDPyr) (1:1 *x*/*x*) membranes have been prepared at the same time and by the same procedures in the S- and R-channels of the cuvette. Negative CH_2 stretching bands in the R-channel reveal a continuous loss of lipids during the time course of the experiment, probably due to electrostatic repulsion between positively charged HDPyr molecules. A significantly higher loss was observed, however, in the presence of LPS as revealed by S-channel spectra and SBSR spectra. The DPPA/(POPC:HDPyr) (1:1 *x*/*x*) membranes lost predominantly the positively charged HDPyr, since equimolar loss of (POPC:HDPyr) would have created a negative C═O double bond stretching band ν(C═O) at 1740 cm^{-1} with approximately half the intensity of $\nu_s(CH_2)$ at 2850 cm^{-1}. Quantitative analysis resulted in total extraction of HDPyr at 1000 μg/mL LPS. Ge IRE; $T = 25$ °C; angle incidence $\Theta = 45°$; number of active internal reflections $N = 36.6 \pm 1$. Buffer: 20 mM sodium phosphate, pH 7.0, 100 mM NaCl.

interacting with 1000 μg of LPS/mL is shown at the top of this figure. The lower trace of each group reflects the absorbance spectrum of the bilayer in contact with LPS, and is referred to as sample S. The trace in the middle results from a DPPA/(POPC:HDPyr) bilayer prepared by the same method and at the same time as S, however contacting only pure buffer. Therefore, it is referred to as reference R. The single channel reference spectra used to calculate the S and R absorbance spectra were recorded before the beginning of the experiment with the lowest LPS concentration. Finally, the upper trace of each group, which is referred to as SBSR, denotes the actual difference S − R. These spectra were measured in the SBSR mode, which means that the sample S and the reference R are placed above each other on the same IRE, thus covering the upper or lower half along the whole length of the plate, respectively. Light is directed alternatively under computer control through the upper half and lower half of the IRE, respectively. S and R cuvettes were separately accessible via tubes, enabling the preparation of the DPPA/(POPC:HDPyr) bilayer at the same time in the R and S cuvettes, however, exposing only the sample S to LPS

Table 2. Quantitative Analysis of Experimental FTIR ATR Data from the Interaction of LPS with a POPC/HDPyr Membrane[a]

part of membrane assembly[b]	integrated absorbance[c]/cm^{-1}		dichroic ratio, R	$\overline{\langle\cos^2\theta\rangle}$	$\bar{\theta}$[d]/deg	$\bar{S}_{CH_2}$[e]	$\bar{S}_{mol}$[f]	Γ[g]/(mol/cm^2)
	∥-pol	⊥-pol						
POPC:HDPyr (1:1 *x*/*x*)	0.4326 ± 0.0050	0.3254 ± 0.0050	1.329 ± 0.026	0.1875 ± 0.0068	64.3 ± 0.5	−0.219 ± 0.010	0.437 ± 0.020	$2.326 \times 10^{-10} \pm 0.152 \times 10^{-10}$
remaining POPC after HDPyr extraction by LPS	0.2658 ± 0.0050	0.1676 ± 0.0050	1.586 ± 0.056	0.2628 ± 0.0086	59.2 ± 0.6	−0.107 ± 0.013	0.212 ± 0.026	$1.939 \times 10^{-10} \pm 0.137 \times 10^{-10}$
extracted HDPyr	0.1064 ± 0.0050	0.1037 ± 0.0050	1.026 ± 0.069	0.0760 ± 0.0037	74.0 ± 0.4	−0.386 ± 0.006	0.772 ± 0.011	$2.042 \times 10^{-10} \pm 0.162 \times 10^{-10}$
POPC of intact DPPA/POPC bilayer	0.1268 ± 0.0050	0.0969 ± 0.0050	1.309 ± 0.085	0.1807 ± 0.0070	64.8 ± 0.5	−0.229 ± 0.010	0.458 ± 0.021	$2.018 \times 10^{-10} \pm 0.191 \times 10^{-10}$

[a] General conditions: germanium IRE, magnitude of parameters see Table 1. [b] The first monolayer attached to the Ge IRE was a DPPA LB layer. [c] Integration range 2830 ± 1 to 2869 ± 1 cm^{-1}. [d] Mean angle between transition moments of $\nu_s(CH_2)$ and the normal to the membrane (*z*-axis). [e] Mean segmental order parameter of methylene groups. [f] The molecular order parameter describes the fluctuation of a molecule with respect to its mean molecular axis. $\bar{S}_{mol} = 1$ means perfect alignment along this axis, $\bar{S}_{mol} = 0$ means isotropic arrangement of molecules. For details see ref 22. [g] Surface concentration as determined by eq 7.

while R remains in contact with buffer. Thus SBSR spectra reflect the instantaneous difference between (POPC:HDPyr)/LPS and (POPC:HDPyr)/buffer, while S and R absorbance spectra report on the whole history of LPS interaction since the measurement of the corresponding reference spectra.

The negative ν(CH) bands of the R spectra in Figure 6 show, unambiguously, that the DPPA/(POPC:HDPyr) bilayer was not absolutely stable during the time course of the experiment. The time to measure the interaction of one concentration of LPS with both polarizations took about 1 1/2 h. At all LPS concentrations, the S spectra reflected a significantly higher lipid loss than the R spectra, which is obviously a consequence of LPS interaction with the positively charged bilayer. Assuming approximately equal spontaneous lipid losses in R and S, then SBSR spectra reflect the lipid loss resulting predominantly from LPS interaction. Obviously, LPS was attracted by the positively charged membrane; however, in contrast to the ATS polymer, LPS was not trapped by the DPPA/(POPC:HDPyr) bilayer but has extracted positively charged HDPyr lipids from the outer monolayer of the membrane.

This finding is substantiated by several observations: First, the nearly complete absence of a ν(C═O) stretching band at 1740 cm^{-1} in the spectra shown in Figure 6 indicates unambiguously the absence of POPC in the extracted lipid. Second, the presence of a sharp negative band near 1495 cm^{-1} resulting from C═C stretching of the aromatic ring of HDPyr (see also Figure 2B) indicates directly the loss of HDPyr. This weak peak is superimposed by a broad shoulder resulting from asymmetric bending of the methyl groups of the choline headgroup of POPC.[34] The bending vibrations $\delta(CH_2)$ of the methylene groups of the hydrocarbon chains appear between 1460 and 1470 cm^{-1}. HDPyr contributed a sharp peak near 1470 cm^{-1} due to its saturated and extended hydrocarbon chains (see below), while $\delta(CH_2)$ of POPC resulted in a broader peak appearing at slightly reduced wavenumbers, due to the less ordered hydrocarbon chains (Figure 2C). As a consequence of HDPyr extraction, there appeared two sharp negative peaks in the SBSR spectra at 1495 and 1470 cm^{-1} as shown in Figure 6. Note that this relevant information is masked in the S spectra by weak uncompensated absorption bands of water vapor, which documents the superior background compensation achieved by the SBSR technique.

A more detailed picture on what has happened upon LPS interaction with the DPPA/(POPC:HDPyr) membrane will now be derived from a quantitative analysis of the observed spectral features. The results of this analysis are summarized in Table 2.

Consider first the negative $\nu_s(CH_2)$ bands at 2850 cm^{-1} in the ∥- and ⊥-polarized SBSR spectra in Figure 6, associated with 1000 μg/mL LPS, which reflect predominantly the loss of HDPyr induced by LPS. The experimental input for this quantitative analysis of extracted HDPyr is based on the determination of the integrated absorbances of $\nu_s(CH_2)$ in the range from 2831 to 2868 cm^{-1}. The results for both polarizations were $a_{\parallel} = 0.1064 \pm 0.0050$ cm^{-1} and $a_{\perp} = 0.1037 \pm 0.0050$ cm^{-1}, respectively, leading to a dichroic ratio of $R_{exp} = a_{\parallel}/a_{\perp} = 1.026 \pm 0.069$. The corresponding mean angle between the transition moment of $\nu_s(CH_2)$, which is oriented along the bisectrice of the H−C−H angle and the normal to the IRE (*z*-axis), can now be evaluated by means of eq 2, resulting in $\bar{\theta} = 74.0° \pm 0.4°$. It should be noted that a perfectly extended (all-trans) hydrocarbon chain which is aligned along the *z*-axis would result in $\bar{\theta} = 90°$, with a corresponding theoretical dichroic ratio for $\nu_s(CH_2)$ of $R_{xy} = 0.858 \pm 0.009$. The other boundary case, namely the isotropic thin film, attached to the IRE, would result in $R_{iso} = 1.88 \pm 0.22$. Therefore, one can conclude that the extracted HDPyr was rather well ordered within the (POPC:HDPyr) layer. According to eq 3 this ordering may also be expressed in terms of the mean segmental order parameter, resulting in $\bar{S}_{CH_2} = -0.386 \pm 0.006$. The perfectly ordered hydrocarbon chain would result in $\bar{S}_{CH_2,perfect} = -0.50$. The surface concentrations Γ corresponding to the four samples under discussion have been calculated by means of eqs 7 and 8 using an integrated molar absorption coefficient for $\nu_s(CH_2)$ of $\int\epsilon(\tilde{\nu})\,d\tilde{\nu} = 5.70 \times 10^5 \pm 0.20 \times 10^5$ cm/mol. The results are summarized in the last column of Table 2.

Discussion

Interaction of LPS with a Clean Ge IRE, a DPPA Monolayer, and an ATS Polymer Network. Only the hydrophilic Ge and, to a greater extent, the positively charged ATS polymer were able to retain some LPS molecules after washing with buffer. The main effect of the endotoxin on the hydrophobic DPPA LB layer was solubilization of DPPA molecules, similar to the action of

(34) Fringeli, U. P.; Günthard, Hs. H. Infrared Membrane Spectroscopy; In *Membrane Spectroscopy*; Grell, E., Ed.; Springer-Verlag: Berlin, Heidelberg, New York, 1981; pp 270−332.

a detergent. It is very unlikely that the protein contamination in our LPS has been responsible for the observed DPPA monolayer destabilization, because LPS/POPC vesicles did not solubilize DPPA, although intense protein adsorption was observed as shown by Figure 5.

Unfortunately, in each case similar amounts of a tightly adsorbed protein were detected. The only explanation for that is contamination of the LPS sample as received from the supplier by one or more highly surface active proteins, which bind quite unspecifically to any surface. We did not change the LPS because of the clinical importance of *Pseudomonas aeruginosa* (serotype 10). However, as a consequence of this disturbance, we felt obliged to estimate the probability that the adsorbed protein could have coated an exposed surface to such an extent that falsification of our conclusions on LPS interaction could be possible. For that purpose the surface concentration of the tightly adsorbed protein was determined from the amide II band in aqueous environment, Figure 5B. It resulted in $\Gamma = 4.00 \times 10^{-10}$ mol of amide groups per cm^2, corresponding to 41.5 Å^2 per amino acid. Theoretically, it would be possible to cover the whole surface by a two-dimensional arrangement of the amino acids, however, since proteins exhibit a three-dimensional structure in general, we assume that there was still enough of free membrane surface for a direct interaction of LPS with the lipid molecules.

Interaction of a Sonicated POPC:LPS (3:1 *x/x*) Mixture with a DPPA LB Layer. This experiment was of special interest since spontaneous adsorption of phospholipids, such as POPC, from vesicular solutions to the hydrophobic surface of a DPPA LB layer is a standard method for performing planar supported bilayers. This method is referred to as the LB/vesicle method.[24] In the presence of LPS, however, POPC was unable to adsorb. Excluding a complete surface coating by a protein contaminant, as discussed in the preceding section, it seems possible that LPS is able to bind significant amounts of POPC, thus keeping POPC in solution which means preventing POPC from adsorption to the hydrophobic surface of a DPPA LB layer.

Interaction of LPS with a DPPA/(POPC:HDPyr) Bilayer. There is unambiguous evidence that the positively charged lipid HDPyr was selectively extracted from the POPC:HDPyr outer monolayer of the supported membrane. Most probably this occurred due to the interaction with LPS and has nothing to do with the protein contaminant. It follows from Table 2, last column, that the POPC:HDPyr layer really consisted of an equimolar mixture of POPC and HDPyr, as originally prepared for adsorption to the DPPA LB layer. After the interaction of the DPPA monolayer with 1000 μg/mL of LPS solution, there was $(1.939 \pm 0.137) \times 10^{-10}$ mol/cm^2 remaining POPC on the IRE and $(2.042 \pm 0.162) \times 10^{-10}$ mol/cm^2 HDPyr has been extracted. Moreover, it can be concluded from the SBSR spectra of extracted HDPyr (Figure 6, top) that these molecules exhibited a high degree of chain ordering in the original layer, as reflected by the corresponding segmental and molecular order parameters $\bar{S}_{CH_2} = -0.386 \pm 0.006$ and $\bar{S}_{mol} = 0.772 \pm 0.011$, respectively. On the other hand, the remaining POPC from the original POPC:HDPyr layer exhibited a reduced chain ordering due to gaps produced upon HDPyr extraction.

Finally, let us consider the initial DPPA/(POPC:HDPyr) membrane (Figure 2B). It has just been shown that POPC and HDPyr were present in equimolar amounts, forming a unit consisting of 47 methylene groups. The corresponding surface concentration according to data listed in Table 2 is found to be $\Gamma = 2.326 \times 10^{-10} \pm 0.152 \times 10^{-10}$ mol·cm^{-2}, which is equivalent to a molecular cross section of 71 ± 4 Å^2. However, such a dense package of the (POPC:HDPyr) unit is not possible since a POPC molecule alone requires this space.[35] The most probable explanation is that more lipid molecules had adsorbed than required for the formation of an oriented densely packed monolayer.

To elucidate this situation, it will be reconstructed from the back. Assuming molecular areas of 70 Å^2 for POPC and 22.5 Å^2 for HDPyr, i.e., 92.5 Å^2 for the (POPC:HDPyr) unit, it follows from the experimentally determined surface concentration of $\Gamma = 2.326 \times 10^{-10} \pm 0.152 \times 10^{-10}$ mol·cm^{-2} that a two-dimensional arrangement of such units would require 1.30 ± 0.09 cm^2. We may conclude that an excess of about 30% (POPC:HDPyr) had absorbed to the DPPA LB layer in the course of membrane preparation. The same calculation was performed at the end of the experimental series. The corresponding spectra are presented in Figure 6, (SBSR; top, 1000 μg/mL). We obtained a mean surface concentration for the (POPC:HDPyr) unit (mean of extracted HDPyr and remaining POPC after HDPyr extraction) of $\Gamma = 1.991 \times 10^{-10} \pm 0.150 \times 10^{-10}$ mol·cm^{-2}, corresponding to an area of 1.11 ± 0.084 cm^2, when taking again molecular cross sections of 70 and 22.5 Å^2 for POPC and HDPyr, respectively. Thus we conclude that there was still an excess of about 10% of lipids at the end of the experiment. It seems that the lipid excess was less tightly bound, because about 20% of the excess material has been washed out during the flow-through experiments with LPS, where increasing concentrations of LPS were pumped through the sample (S) cuvette. Simultaneously, pure buffer was pumped through the reference (R) cuvette. We suggest that the lipid excess consists of small membrane fragments from the vesicular solution used for the membrane preparation. Such a behavior is known from earlier experiments with bilayer formation;[19] however, surface cleaning was in general possible by applying a so-called "air piston", i.e., draining the cuvette followed by immediate refilling.[24] Loosely bound lipids could then be washed out. In this application, loosely bound lipids were assumed to exhibit random orientation further on.

On the basis of this interpretation, we can use eqs 4 and 5 to calculate $\langle\cos^2\theta\rangle^{layer}_{HDPyr}$, and the corresponding dichroic ratio R^{layer}_{HDPyr}. The mole fractions are $x^{layer}_{HDPyr} = 0.90$ and $x^{random}_{HDPyr} = 0.10$, as follows from the required two-dimensional total surface of $A_{total} = 1.11 \pm 0.084$ cm^2 for POPC and HDPyr (1:1 *x/x*) immediately before the interaction with the highest LPS concentration. The mean dichroic ratio $R_{exp} = \langle R\rangle = 1.026 \pm 0.069$, as determined from the SBSR spectra in Figure 6 top is thus composed of R^{layer}_{HDPyr}, featuring 90% of the substance, and R^{random}_{HDPyr}, featuring the assumed loosely bound remaining 10% of HDPyr. It follows from eq 4 for HDPyr that

$$\langle R\rangle = \frac{0.9\langle d_{e,\parallel}\rangle^{layer}_{HDPyr} + 0.1\langle d_{e,\parallel}\rangle^{random}_{HDPyr}}{0.9\langle d_{e,\perp}\rangle^{layer}_{HDPyr} + 0.1\langle d_{e,\perp}\rangle^{random}_{HDPyr}} \qquad (9)$$

Replacing now the effective thicknesses in eq 9 by eq 5 and taking into account $\langle\cos^2\theta\rangle^{random}_{HDPyr} = 1/3$, as well as that expressions for $\langle d_{e,\parallel}\rangle_{iso}$ and $\langle d_{e,\perp}\rangle_{iso}$ are available from literature,[18-22] it follows that the only unknown in eq 9 is $\langle\cos^2\theta\rangle^{layer}_{HDPyr}$, which is found to be $\langle\cos^2\theta\rangle^{layer}_{HDPyr} = 0.0475 \pm 0.0044$. This value corresponds to a mean angle between the transition moments of $\nu_s(CH_2)$ and the *z*-axis of $\bar{\theta}^{layer}_{HDPyr}$

(35) Rand, R. P. *Annu. Rev. Biophys. Bioeng.* **1981**, *10*, 277.

Table 3. Orientation Analysis of Experimental Data of the DPPA/(POPC:HDPyr) Membrane Assembly[a]

component	molecular mole fraction	methylene group mole fraction	dichroic ratio, R	$\overline{\langle\cos^2\theta\rangle}$	$\bar{\theta}$[b]/deg	$\bar{S}_{CH_2}$[c]	$\bar{S}_{mol}$[d]
HDPyr in layer	0.385	0.200	0.96 ± 0.01	0.0475 ± 0.0044	77.4 ± 0.4	−0.429 ± 0.07	0.857 ± 0.013
POPC in layer	0.385	0.426	1.15 ± 0.10	0.1251 ± 0.0392	69.3 ± 0.7	−0.312 ± 0.059	0.625 ± 0.117
(POPC:HDPyr) loosely bound[e]	0.230	0.374	1.88 ± 0.22	0.3333	54.7	0	0

[a] The evaluation is based on the overall dichroic ratio of $\nu_s(CH_2)$, $R_{exp} = 1.329$ as determined from Figure 2B, before LPS interaction, and on the dichroic ratio of $\nu_s(CH_2)$ of extracted HDPyr, $R_{exp} = 1.026$, Figure 6, top. Separation of superimposed structures was performed by means of eq 4. For details see text. [b] Mean angle between transition moments of $\nu_s(CH_2)$ and the normal to the membrane (z-axis). [c] Mean segmental order parameter of methylene groups. [d] Mean molecular order parameter of methylene groups. [e] Isotropic arrangement of methylene groups was assumed.

$= 77.4° \pm 0.4°$. The dichroic ratio results in from eq 5 $R^{layer}_{HDPyr} = \langle d_{e,||}\rangle^{layer}_{HDPyr}/\langle d_{e,\perp}\rangle^{layer}_{HDPyr} = 0.96 \pm 0.01$, corresponding to segmental and molecular order parameters of $S^{layer}_{CH_2,HDPyr} = -0.429 \pm 0.07$, and $S^{layer}_{mol,HDPyr} = 0.857 \pm 0.013$. Of course, there is no definite proof for this interpretation, which is based on the ultrastructural model of a planar supported bilayer and randomly adsorbed membrane fragments. However, the following check will show that this model is very reasonable. Consider the superposition of three populations of molecular ordering in the initial (POPC:HDPyr) layer: HDPyr in the layer, as just discussed; POPC in the layer, reflecting an unknown ordering; and (POPC:HDPyr) loosely bound to the membrane surface, featuring random orientation of methylene groups. The overall dichroic ratio was experimentally accessible from Figure 2B and resulted in, according to Table 2, $R = 1.329 \pm 0.026$. The mole fractions of oriented layer and randomly adsorbed lipid resulted in for the initial (POPC:HDPyr) layer $x^{layer} = 0.770$ and $x^{random} = 0.230$, respectively, as concluded from the required two-dimensional area of $A_{total} = 1.30 \pm 0.09$ cm^2 at the beginning of the experiment. Both components were found to be equimolar, thus $x^{layer}_{HDPyr} = 0.385$, $x^{layer}_{POPC} = 0.385$, and for the loosely bound complex $x^{random}_{HDPyr:POPC} = 0.230$. These mole fractions are referred to as molecular mole fractions. To get the mole fractions to be introduced into eq 4 referred to as "functional group" mole fractions, one has to take the number of methylene groups in each of the three populations into account. Denoting the number of methylene groups in a molecule of the kth population by ν_k ($k = 1, 2, 3$), then the conversion of molecular mole fractions x_k(molec) into "functional group" mole fractions x_k(fcgrp) is given by

$$x_k(\text{fcgrp}) = \frac{\nu_k x_k(\text{molec})}{\sum_{k=1}^{3} \nu_k x_k(\text{molec})} \qquad (10)$$

Assigning HDPyr in the layer to $k = 1$, POPC in the layer to $k = 2$, and surface-bound random (POPC:HDPyr) unit to $k = 3$, then it follows with $\nu_1 = 15$, $\nu_2 = 32$, and $\nu_3 = 47$ for the corresponding "functional group" mole fractions x_1(fcgrp) = 0.200, x_2(fcgrp) = 0.426, and x_3(fcgrp) = 0.374. Setting the relative transition moments $m_k = 1$, and the mean square cosines as determined earlier to $\overline{\langle\cos^2\theta\rangle}^{layer}_{HDPyr} = 0.0475 \pm 0.0044$, and $\overline{\langle\cos^2\theta\rangle}^{random}_{(POPC:HDPyr)} = 0.3333$ (see Table 3), the only unknown remaining in eq 4 is the mean square cosine of the angle between transition moments of $\nu_s(CH_2)$ and the z-axis, $\overline{\langle\cos^2\theta\rangle}^{layer}_{POPC}$. Using the values for axial effective thicknesses of an isotropic layer, as indicated in the Theoretical Section, and the overall dichroic ratio of the initial layer, $R_{exp} = 1.329 \pm 0.026$, it followed that $\overline{\langle\cos^2\theta\rangle}^{layer}_{POPC} = 0.1251 \pm 0.0392$, leading to $\bar{\theta}^{layer}_{POPC} = 69.3° \pm 0.7°$. According to eq 1 the dichroic ratio of POPC in the oriented layer was calculated to be $R^{layer}_{POPC} = 1.15 \pm 0.10$, or expressed in terms of the segmental order parameter according to eq 3, $\bar{S}^{layer}_{CH_2,POPC} = -0.312 \pm 0.059$, which corresponds to a molecular order parameter of $\bar{S}^{layer}_{mol,POPC} = 0.625 \pm 0.117$. The results of this theoretical analysis are summarized in Table 3. It should be noted that, according to this analysis, POPC in the layer reflects a rather high chain ordering when compared to the pure POPC monolayer presented for the sake of comparison in Figure 2C. The mean molecular cross section of a POPC molecule, as calculated from the surface concentration, results in 82.3 ± 7.5 Å^2, which is at the upper limit of a closely packed POPC monolayer.[35] Two reasons for the high degree of POPC chain ordering in the (POPC:HDPyr) layer may be mentioned: first, enhanced alignment due to incorporation of the stiffer hydrocarbon chains of HDPyr and, second, a not completely fulfilled assumption that lipid molecules loosely bound to the (POPC:HDPyr) layer exhibit a random chain ordering. In the latter case POPC in the layer would have to assume a lower chain ordering than calculated here, to achieve the experimentally determined overall dichroic ratio of $R = 1.329 \pm 0.026$.

Conclusions

It has been shown that LPS from *Pseudomonas aeruginosa* (serotype 10) interacted preferentially with positively charged surfaces such as aminopropyltriethoxysilane (ATS) and lipid bilayer membranes containing positively charged lipid molecules such as hexadecylamine (HDA), hexadecylpyridinium (HDPyr), and hexadecyltrimethylammonium (HDTMA). While LPS was trapped by the ATS polymer network, it was able to extract HDA, HDPyr, and HDTMA completely from a mixed monolayer containing palmitoyloleoylphosphatidylcholine (POPC) and one of the positively charged lipid in equimolar amounts.

A highly surface active protein as a contaminant of LPS from *Pseudomonas aeruginosa* (not specified by the supplier) was found to adsorb irreversibly to all surfaces under inspection. A quantitative estimation of the surface coverage, as well as the different responses of surfaces to LPS interaction showed, however, that the disturbance of the contaminant was not significant.

LPS exhibited a detergent-like behavior when interacting with the hydrophobic surface of a dipalmitoylphosphatidic acid (DPPA) LB layer. The normally very stable DPPA layer was partly detached from the internal reflection plate, which acted as solid support. On the other hand, destabilization of the DPPA LB layer was not observed in the presence of mixed POPC/LPS vesicles. Obviously, POPC was hindered from adsorbing spontaneously to the DPPA monolayer under these conditions, but

on the other hand LPS was hindered by POPC from destabilizing the DPPA monolayer.

Most spectroscopic effects in connection with LPS interaction have been analyzed quantitatively in terms of surface concentration, orientation, and ultrastructure of the membrane assembly.

Glossary

ATR	attenuated total reflection
ATS	aminopropyltriethoxysilane
DPPA	dipalmitoylphosphatidic acid
FTIR	Fourier transform infrared
HDA	hexadecylamine
HDPyr	hexadecylpyridinium
HDTMA	hexadecyltrimethylammonium
IRE	internal reflection element
LB	Langmuir−Blodgett
LPS	lipopolysaccharide
POPC	palmitoyloleoylphosphatidylcholine
SBSR	single-beam-sample-reference

Acknowledgment. The authors thank the Austrian National Bank (OeNB) for continuous financial support of endotoxin research by Project Nos. 7530-1 and 7530-2.

LA011662K